



Measured sound speeds and acoustic nonlinearity parameter in liquid water up to 523 K and 14 MPa

Blake T. Sturtevant, Cristian Pantea, and Dipen N. Sinha

Citation: *AIP Advances* **6**, 075310 (2016); doi: 10.1063/1.4959196

View online: <http://dx.doi.org/10.1063/1.4959196>

View Table of Contents: <http://scitation.aip.org/content/aip/journal/adva/6/7?ver=pdfcov>

Published by the *AIP Publishing*

Articles you may be interested in

Density measurements of subcooled water in the temperature range of (243 and 283) K and for pressures up to 400 MPa

J. Chem. Phys. **144**, 074501 (2016); 10.1063/1.4941580

The acoustic nonlinearity parameter in Fluorinert up to 381 K and 13.8 MPa

J. Acoust. Soc. Am. **138**, EL31 (2015); 10.1121/1.4922537

The speed of sound and derived thermodynamic properties of pure water at temperatures between (253 and 473) K and at pressures up to 400 MPa

J. Chem. Phys. **136**, 094511 (2012); 10.1063/1.3688054

Speed of sound instrument for fluids with pressures up to 100 MPa

Rev. Sci. Instrum. **77**, 123903 (2006); 10.1063/1.2400019

Water as a standard in the measurements of speed of sound in liquids

J. Acoust. Soc. Am. **102**, 2776 (1997); 10.1121/1.420332

The advertisement features a blue and orange background with a molecular structure graphic. On the left is a thumbnail of an 'Applied Physics Reviews' journal cover. The main text reads 'NEW Special Topic Sections' in large white font. Below this, it says 'NOW ONLINE' in orange, followed by 'Lithium Niobate Properties and Applications: Reviews of Emerging Trends' in white. The AIP Applied Physics Reviews logo is in the bottom right corner.

NEW Special Topic Sections

NOW ONLINE
Lithium Niobate Properties and Applications:
Reviews of Emerging Trends

AIP Applied Physics Reviews

Measured sound speeds and acoustic nonlinearity parameter in liquid water up to 523 K and 14 MPa

Blake T. Sturtevant,^a Cristian Pantea, and Dipen N. Sinha
*Materials Physics and Applications, Los Alamos National Laboratory,
 Los Alamos, NM USA 87545*

(Received 13 June 2016; accepted 8 July 2016; published online 15 July 2016)

Sound speed in liquid water at temperatures between 275 and 523 K and pressures up to 14 MPa were experimentally determined using a high temperature/high pressure capable acoustic resonance cell. The measurements enabled the determination of the temperature and pressure dependence of sound speed and thus the parameter of acoustic nonlinearity, B/A , over this entire P - T space. Most of the sound speeds measured in this work were found to be within 0.4% of the IAPWS-IF97 formulation, an international standard for calculating sound speed in water as a function of temperature and pressure. The values for B/A determined at laboratory ambient pressure and at temperatures up to 356 K, were found to be in general agreement with values calculated from the IAPWS-IF97 formulation. Additionally, B/A at 293 K was found to be 4.6, in agreement with established literature values. © 2016 Author(s). All article content, except where otherwise noted, is licensed under a Creative Commons Attribution (CC BY) license (<http://creativecommons.org/licenses/by/4.0/>). [<http://dx.doi.org/10.1063/1.4959196>]

I. INTRODUCTION

Sound speed in a medium as a function of temperature and pressure plays an important role in both basic and applied research. From a basic research perspective, sound speed measured over a range of temperatures and pressures can be used in constructing and refining equations-of-state (EOS) for a medium.^{1,2} Because sound speed is a derivative quantity, small changes in its value can significantly impact the free energies calculated from EOS models. Careful measurement of sound speed spanning a wide range of temperatures and pressures thus puts strict limits on EOS parameters. Additionally, knowledge of sound speed dependence on temperature and pressure is one popular method of determining acoustic nonlinearity in a medium.^{3,4} Acoustic nonlinearity is an inherent physical property of materials and has been targeted in technological applications such as harmonic imaging and parametric sonar imaging.⁵⁻⁹ The acoustic nonlinearity of homogenous isotropic media is often described by the ratio of coefficients, B/A , in the isentropic equation of state. This EOS relates the pressure, P , and the mass density, ρ , through a simple expansion (subscript '0' indicates an unperturbed ambient quantity):³

$$P - P_0 = A \frac{\rho - \rho_0}{\rho_0} + \frac{B}{2} \left(\frac{\rho - \rho_0}{\rho_0} \right)^2 + \dots \quad (1)$$

In 1960, Beyer described the now popular thermodynamic method for experimentally determining B/A :³

$$\frac{B}{A} = 2\rho_0 c_0 \left(\frac{\partial c}{\partial P} \right)_T + \frac{2c_0 T \alpha_v}{C_p} \left(\frac{\partial c}{\partial T} \right)_P = \left(\frac{B}{A} \right)' + \left(\frac{B}{A} \right)'' \quad (2)$$

Equation (2) relates B/A to the pressure and temperature derivatives of sound speed, c , as well as the mass density, the coefficient of volumetric thermal expansion (α_v), the isobaric specific heat

^aCorresponding author. Email: bsturtev@lanl.gov

(C_p), and the absolute (kelvin) temperature, T . As in Eqn. (1), the ‘0’ subscript in Eqn. (2) indicates the property value at the unperturbed temperature and pressure (i.e. the temperature or pressure at which the pressure or temperature derivative is calculated, respectively). For brevity, (B/A)’ and (B/A)” will subsequently be used to refer to the pressure derivative and temperature derivative terms of Eqn. (2), respectively.

In addition to the thermodynamic method, a second commonly used technique for quantifying acoustic nonlinearity is the *finite amplitude (FA) method*.^{9–11} In the FA method, an acoustic wave of a particular frequency, f_1 , is launched in a nonlinear medium and the amplitude of the second harmonic with frequency $2 \cdot f_1$ is recorded. The more nonlinear a medium is, the higher the observed amplitude of the second (and higher) harmonic. The parameter of nonlinearity reported in FA studies is most often β which is simply related to B/A :

$$\beta = 1 + \frac{B}{2A}. \quad (3)$$

The thermodynamic and finite amplitude methods have previously been shown to yield extracted B/A parameters in agreement with each other and the technique that one uses is determined by experimental logistics.¹⁰

Several authors have previously reported experimental determinations of B/A in liquid water at room temperature and pressure with at least three authors reporting values for this quantity at temperatures up to 100°C.^{3,11–16} The present work is motivated in part by the need to determine B/A at higher temperatures to enable technological applications in downhole geothermal or petroleum boreholes. The 523 K temperature limit of this work was chosen because it is representative of the higher temperatures observed at depths up to 10 km in the continental United States.¹⁷ A previously reported high temperature/high pressure acoustic resonance cell¹⁸ enabled the measurement of sound speed at 18 temperatures between 275 K and 523 K and at 11 pressures between 76 kPa and 13.8 MPa.

Section II presents a brief derivation of the thermodynamic method for determining B/A . Section III reviews the experimental data collection while Section IV describes the sound speed and B/A analysis procedure. Section V discusses the results of this work, placing them in the context of published literature and Section VI concludes the paper.

II. THEORETICAL

Equation (2) is often cited in the literature without derivation.²⁴ This section presents a brief derivation of the thermodynamic method for determining B/A , Eqn. (2), from the isentropic equation of state given in Eqn. (1). At conditions of constant entropy, S , the instantaneous pressure, P , can be expanded about its equilibrium value, P_0 , using a second order Taylor expansion in the instantaneous density, ρ :

$$P - P_0 = \left(\frac{\partial P}{\partial \rho} \right)_S (\rho - \rho_0) + \frac{1}{2!} \left(\frac{\partial^2 P}{\partial \rho^2} \right)_S (\rho - \rho_0)^2. \quad (4)$$

Comparing Eqn. (1) with Eqn. (4), it is seen that:

$$A = \rho_0 \left(\frac{\partial P}{\partial \rho} \right)_S \quad \text{and} \quad B = \rho_0^2 \left(\frac{\partial^2 P}{\partial \rho^2} \right)_S.$$

By definition:¹⁹

$$c_0^2 = \left(\frac{\partial P}{\partial \rho} \right)_S, \quad (5)$$

leading to the following expression for B/A :

$$\frac{B}{A} = \frac{\rho_0}{c_0^2} \left(\frac{\partial^2 P}{\partial \rho^2} \right)_S. \quad (6)$$

Differentiation of Eqn. (5) with respect to the density enables Eqn. (6) to be rewritten as:

$$\frac{B}{A} = 2\rho_0 c_0 \left(\frac{\partial c}{\partial P} \right)_S. \quad (7)$$

Previous works have used Eqn. (7) to determine B/A by measuring experimentally determining $\left(\frac{\partial c}{\partial P}\right)$ under isentropic conditions.^{12,13} In the present work, isothermal and isobaric conditions were more easily and reliably achieved than isentropic conditions. A change of variables from pressure and entropy to pressure and temperature, enables the derivative in Eqn. (7) to be rewritten:

$$\left(\frac{\partial c}{\partial P} \right)_S = \left(\frac{\partial c}{\partial P} \right)_T + \left(\frac{\partial c}{\partial T} \right)_P \left(\frac{\partial T}{\partial P} \right)_S. \quad (8)$$

The two derivatives of c on the right hand side (R.H.S) of Eqn. (8) are easily determined experimentally while the isentropic pressure derivative of temperature can be rewritten using the Maxwell relation for the enthalpy and then expanding the resulting derivative:

$$\left(\frac{\partial T}{\partial P} \right)_S = \left(\frac{\partial V}{\partial S} \right)_P = \left(\frac{\partial V}{\partial T} \right)_P \left(\frac{\partial T}{\partial S} \right)_P. \quad (9)$$

The two derivatives on the R.H.S of Eqn. (9) are identified as:

$$\left(\frac{\partial V}{\partial T} \right)_P = V\alpha_v, \text{ and } \left(\frac{\partial T}{\partial S} \right)_P = \frac{m}{T} C_p \quad (10)$$

where m and V are mass and volume elements, respectively. Successive substitution of Eqn. (10) into Eqn. (9), of Eqn. (9) into Eqn. (8), and of Eqn. (8) into Eqn. (7) leads directly to Eqn. (2).

III. EXPERIMENTAL

A. Swept Frequency Acoustic Interferometry Technique (SFAI)

The sound speed in water was determined from measured transmission frequency spectra using the Swept Frequency Acoustic Interferometry (SFAI) technique and the specially designed acoustic resonance cell mentioned above. The technique and the measurement cell are detailed in Refs. 18 and 20 respectively. Briefly, a transmitting transducer is excited using a frequency that is swept over a frequency range of interest. A separate receiving transducer is used to record a resonance spectrum consisting of multiple equally spaced resonant frequencies, f_n , through a vector network analyzer or its functional equivalent. For a one dimensional cavity constructed of perfectly hard walls separated by a distance L , acoustic resonances are observed for displacement waves with nodes at the cavity boundary (i.e. the wavelength, $\lambda_n = 2 \cdot L/n$ for the n^{th} harmonic). When this criterion is combined with the wave relationship, $c = \lambda_n f_n$, one finds the following relationship between sound speed, path length, and the spacing of adjacent resonances in the frequency domain:

$$c = 2L \frac{df_n}{dn}. \quad (11)$$

B. Measurement Cell and Sample Environment

Figure 1 presents a schematic of the experimental setup consisting of the measurement cell, high T/P environment, and PC-controlled network analyzer. The acoustic resonance cell used to determine sound speed in this work consists of a pair of pure-longitudinal mode single crystal lithium niobate transducers that are housed in stainless steel enclosures to protect them from the high temperature aqueous environment.²⁰ The physical dimension, L , of the resonant cavity fluid path length was calibrated at 76 kPa and 293 K using the speed of sound in distilled water measured by a commercially available sound velocity meter (Anton-Paar DSA 5000 M) and found to be $L = 8.873 \pm 0.003$ mm. Our laboratory is positioned at 2250 meters above sea level and has an annual average air pressure of 76 kPa, significantly lower than the average atmospheric pressure of

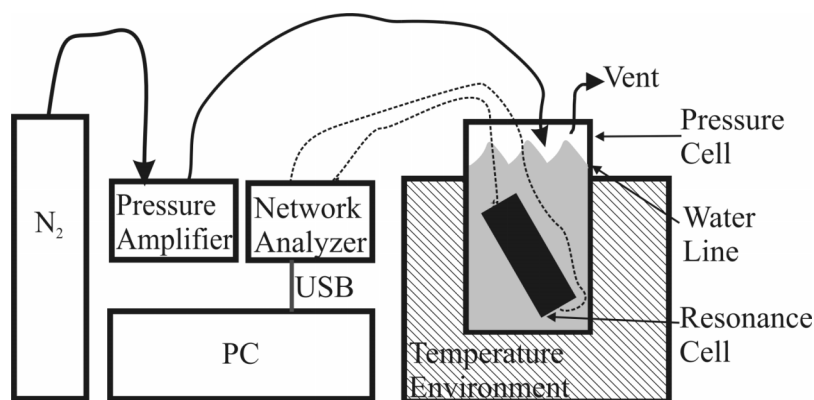


FIG. 1. Schematic of the experimental setup. The high temperature/pressure resonance cell, detailed in Fig. 1, is immersed in water inside a high pressure cell. The headspace of the pressure cell is pressurized using N₂ from a gas cylinder through a pressure amplifier. High pressure gas lines are represented with solid black arrowed lines while signal carrying coaxial cables are represented using dashed lines.

101.4 kPa at sea level. Thermal expansion in the 304 stainless steel spacers that determine L was accounted for using coefficients of thermal expansion of 17.2 ppm/K and 17.8 ppm/K at temperatures between 273-373 K and 373-523 K, respectively.²¹

The high temperature/ high pressure measurement environment was provided by a commercially available pressure vessel (model# 4681, Parr Instrument Company, Moline, IL). The resonance cell, occupying a volume of ~ 100 mL, was placed inside the 1-liter pressure vessel along with 700 mL of degassed, deionized water (see Fig. 1). The headspace in the pressure vessel consisted of nominally whole air and was pressurized with nitrogen gas using a pressure amplifier (Model: AAD-30, Haskel International, Inc., Burbank, CA) to achieve the hydrostatic pressure conditions in this study. The temperature environment shown in Fig. 1 consisted of a 4-gallon temperature controlled bath for temperatures below 350 K and of a fitted furnace for temperatures between 350 K and 523 K.

C. Data Collection

Data were collected at 18 temperatures between 275 K and 523 K. A type-J thermocouple was used to determine the temperature of the sample environment with a precision of ± 0.1 K and an accuracy of 1.1 K. The thermocouple was carefully positioned as close as possible to the resonance cavity to reduce any bias associated with thermal gradients inside the pressure vessel. Once the temperature in the sample environment had stabilized to within 0.1 K and remained stable for a period of several minutes, an SFAI spectrum was collected at the target temperature and at a pressure corresponding to the water liquid-vapor coexistence boundary at that temperature. The frequency-sweep spectrum collection took approximately one minute. If the temperature read by the thermocouple changed by 0.1 K or more during the course of spectrum collection, the system was allowed to further stabilize and the spectrum was recollected. The system was then pressurized to 13.79 MPa and again allowed to thermally equilibrate before a spectrum was collected. Following the recording of a spectrum, the pressure in the vessel was reduced by 1.379 MPa by venting the headspace through a needle valve over a period of approximately one minute. This sequence of venting, equilibration, and spectrum collection was repeated at up to 11 equally spaced pressures between the upper limit of 13.79 MPa and the lower limit determined by the water vapor pressure at the target temperature. Temperature changes of up to a couple kelvin were observed between laboratory ambient pressure and 13.8 MPa due to the compression of gas in the vessel headspace. Here, “ambient” refers to the lowest pressure achievable at each temperature and is the sum of the laboratory air pressure and the vapor pressure of water as read by the attached pressure gage. A 0-34.5 MPa pressure transducer (Model PX309-5KG5V, Omega Engineering, Inc.) was used to

determine the pressure inside the vessel at each data point with a precision of ± 3.4 kPa and a manufacturer-reported accuracy of 90 kPa.

The resonance spectra (S_{21} forward transmission scattering parameter) were recorded using a vector network analyzer (Model Bode 100, OMICRON electronics Corp. USA, Houston TX), shown schematically in Fig. 1. The signals between the resonance cell and network analyzer were carried over stainless steel-sheathed coaxial cables that could withstand high temperatures and that allowed for an air tight seal to be made with the pressure vessel using Swagelok compression fittings. At each temperature and pressure, 6401 frequency points were recorded with a 1 kHz receiver bandwidth between 1 MHz and 8 MHz at a source power of 0 dBm.

IV. ANALYSIS

At each temperature and pressure combination, Eqn. (11) was used to determine the sound speed from the measured frequency spectra along with a temperature-adjusted path length, L , as described in Ref. 20. In the analysis procedure, multiple successive resonance frequencies are plotted against the cycle number, n , and a linear fit is performed to determine df_n/dn and its associated uncertainty.

To determine B/A from Eqn. (2), it is necessary to know how sound speed in a medium depends on temperature as well as on pressure. To calculate the necessary derivatives, the data were binned into nominal isobars and isotherms and then fit with differentiable functions. Polynomials are commonly chosen for this due to their ease of implementation and the achievable goodness of fit. In polynomial fitting, it must be kept in mind that the values of polynomial, and its derivative, can be very sensitive to the value of boundary data points. In this work, the lowest order polynomials that successfully captured all features of the data were selected. The temperature behavior required a sixth-order polynomial while the pressure changes were found to be accurately modeled with a quadratic polynomial.

A polynomial that was sixth order in temperature was fit to each set of isobaric data and differentiated to determine dc/dT at each temperature and pressure combination:

$$c(T, P) = a_{00} + a_{01}(P - P_0) + a_{10}T + a_{20}T^2 + a_{30}T^3 + a_{40}T^4 + a_{50}T^5 + a_{60}T^6. \quad (12)$$

The a_{01} term in the polynomial was used to account for the fact that the pressures at each data point were not exactly the same, being limited by the precision with which the headspace could be vented through the needle valve. Because none of the pressures deviated appreciably from the mean, P_0 , a linear term sufficed to account for the difference.

For water, roughly 95% of B/A is attributable to the $(B/A)'$ term and thus an accurate determination of $\frac{\partial c}{\partial P}$ is very important. To determine the pressure dependence of sound speed, the measured sound speeds were binned into 18 nominally isotherms. It was necessary to account for the temperature difference associated with pressurizing the vessel's headspace, as mentioned above. For a small temperature range such as observed here (2 K), it can be safely assumed that sound speed varies linearly with temperature. Thus, a linear temperature term was included in the polynomial used to fit the nominally isothermic data:

$$c(T, P) = b_{00} + b_{10}(T - T_0) + b_{01}P + b_{02}P^2. \quad (13)$$

Initial fits using a polynomial of the form of Eqn. (13) indicated that letting b_{10} vary unconstrained resulted in linear temperature coefficients which were unrealistic based on the fits to isothermal data performed above. As a result, when fitting the pressure polynomial, the temperature behavior calculated from fitting Eqn. (12) were used for b_{10} at each isobar. Thus, all data in the nominal isotherm were corrected to be exactly isothermal with temperature T_0 prior to determining the pressure dependence. Additionally, the zero intercept term, b_{00} was constrained to ensure that the fit passed through the sound speed at the lowest measured pressure at each temperature. The sound speeds measured by SFAI at the lowest pressures between 275 and 343 K were measured independently by a commercial Anton-Paar instrument and found to be in good agreement, indicating that confidence in these data points was justified. Imposing this constraint on the polynomial fit

greatly helped to mitigate the boundary effects of polynomial fitting mentioned above. Finally, the b_{01} and b_{02} coefficients in Eqn. (14) were determined using a least squares fit. To ensure that $\frac{\partial c}{\partial P}$ was determined as accurately as possible, outliers more than two standard deviations away from the fit (2σ , 95% confidence interval) were discarded and the polynomials were recalculated, if necessary. Four percent of the 203 measured data points obtained were discarded based on this criterion which can be expected for normally distributed random errors. The b_{01} and b_{02} coefficients were then used to calculate $\frac{\partial c}{\partial P}$ at each temperature and pressure.

The experimentally determined sound speeds were compared to those calculated from an internationally accepted standard equation of state for water, the IAPWS-IF97 formulation.^{22,23} This dataset was used as a basis for comparison since there are no experimental data published over the entire temperature and pressure range considered in this work. The IAPWS-IF97 calculates sound speed (and other thermodynamic properties) through derivatives of the dimensionless specific Gibbs free energy. The dimensionless Gibbs free energy is expressed in IAPWS-IF97 through a *basic equation* consisting of a 34 term polynomial in dimensionless temperatures and pressures. The coefficients and orders of the basic equation's polynomial are determined from experimentally determined, "thermal properties of the single-phase region ($P\rho T$), [...] specific isochoric heat capacity, specific isobaric heat capacity, speed of sound, differences in the specific enthalpy and in the specific internal energy, Joule-Thomson coefficient, and isothermal throttling coefficient."²³ The basic equation is reported to be valid for temperatures between 251.2 and 1273 K and pressures up to 1000 MPa.²³ The IAPWS-IF97 formulation was used to calculate sound speeds for every temperature and pressure combination for which an experimental sound speed was determined. Analogous to Eqns. (12) & (13), the temperature and pressure dependence of the IAPWS-IF97 data were determined from a single polynomial which was sixth order in temperature and third order in pressure (and included cross terms):

$$c(T, P) = \sum_{i=0}^6 \sum_{j=0}^3 a_{ij} P^j T^i. \quad (14)$$

Since the IAPWS-IF97 sound speeds are, in fact, calculated from a polynomial, they were expected to be smooth and continuous in P - T space, allowing them to be fit well with a single, two variable polynomial, rather than piecewise in T and P as with the experimental data described above. The inclusion of the cross terms reflects the dependence of temperature behavior on pressure, and vice versa. This dependence is accounted for in the experimental data by fitting the data piecewise with no restriction that the temperature behavior must be the same among different isobars or that the pressure behavior must be the same for different isotherms. The mass density and isobaric specific heat capacity needed to determine B/A , were also calculated from the IAPWS-IF97. Additionally, the volumetric coefficient of thermal expansion, α_v , was calculated from the density data through the relationship $\alpha_v = (-1/\rho) * d\rho/dT$. These thermodynamic properties were combined with the temperature and pressure dependence of both the experimental sound speed as well as with the IAPWS-IF97 predicted sound speed to calculate B/A at all temperatures and pressures studied.

V. RESULTS AND DISCUSSION

A. Sound Speed

As an independent verification of the described experimental and analysis procedure, sound speeds at laboratory pressure and at temperatures up to 360 K were compared to those measured with an Anton-Paar commercially available sound speed meter mentioned above. These two data sets are compared in Fig. 2 and are seen to be in good agreement. When a 6th order polynomial was fit to the Anton-Paar data, the SFAI determined sound speeds all agreed with this fit to within 0.4%. The manufacturer states the accuracy of the DSA 5000 M is ± 0.5 m/s, or $\sim 0.03\%$ for the sound speeds considered here.

All sound speeds measured in this work are tabulated in the [Supplementary Material](#). Figure 3 presents these data in the form of a contour plot to highlight two general trends. First, the unusual but well-known maximum in water sound speed at temperatures near 350 K is observed.

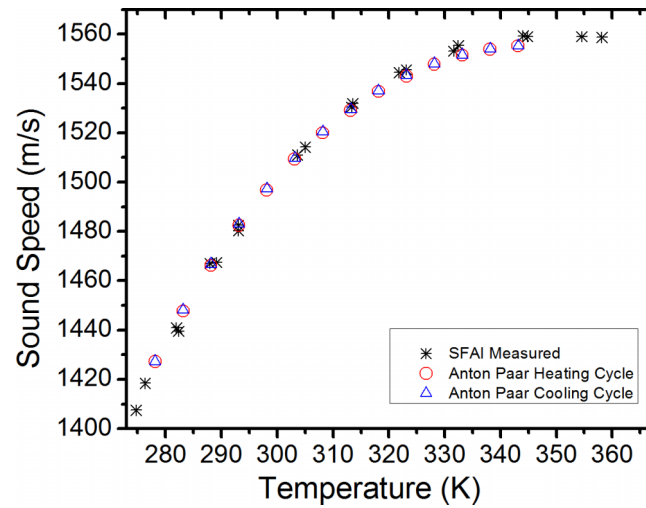


FIG. 2. Comparison of sound speed measured by the measurement cell used in this work and sound speed measured by a commercial sound speed measurement system, Anton-Paar DSA 5000M, at laboratory ambient pressure.

Sound speed at laboratory pressure was observed to increase from its 275 K value by 11% to a maximum of 1559 m/s near 350 K. After passing through this maximum, sound speed monotonically decreased to a value of 1155 m/s at 522 K. Secondly, sound speed can be seen to increase with pressure at all temperatures. Over the 14 MPa pressure range studied here, sound speed increased by ~ 20 m/s between the lowest and highest pressures at a given temperature.

The uncertainty associated with the determination of the resonant cavity length, L , and resonance frequency spacing df_n/dn led to a precision of $\sim 0.05\%$ in the determined sound speeds. The 0.05% precision was determined by the standard error of the linear fit coefficient used to determine df_n/dn . The precision in L is determined by the precision of the temperature measurement (0.1 K) and the coefficient of thermal expansion, ~ 20 ppm/K, and is over an order of magnitude less than the uncertainty in df_n/dn . While the precision in sound speed is determined by the precision of df_n/dn , the accuracy of the measured sound speeds is primarily attributable to the accuracy of the temperature measurement. The ± 1.1 K uncertainty in temperature mentioned above has a variable effect on the uncertainty in sound speed, depending on the temperature being considered. For example, in the vicinity of the sound speed maximum near 350 K, temperature has a minimal effect

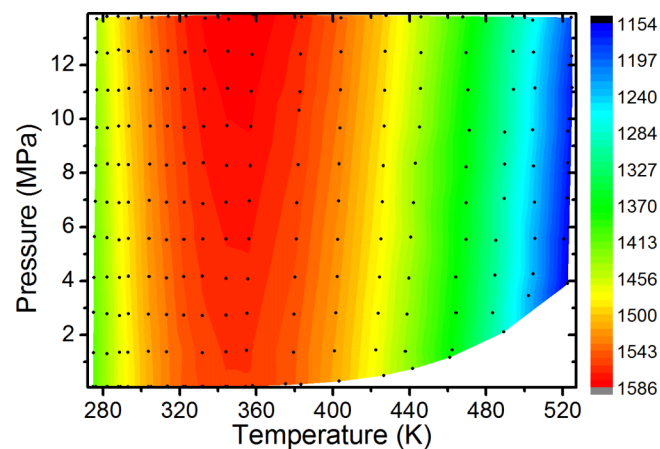


FIG. 3. Contour plot of the measured sound speeds (m/s) as a function of temperature and pressure. Significant features such as the maximum of sound speed near 350 K as well as the increase of sound speed with pressure are observed. Filled circles indicate measurement points.

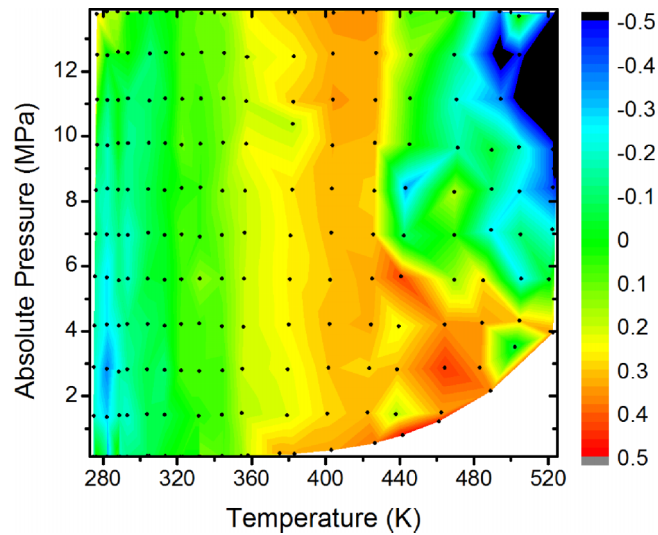


FIG. 4. Map of Temperature-Pressure space showing the difference between IAPWS-IF97 predicted sound speeds and the sound speeds measured in this work, expressed as a percent of the measured value. Filled circles denote measurement points.

on sound speed and so the uncertainty in temperature does not significantly affect the uncertainty in the determined $c(P,T)$. However, at the higher and lower temperatures considered here, $\frac{\partial c}{\partial T}$ can be as large as $\pm 3\text{-}4$ m/s/K. In these regions, uncertainty in the temperature measurements impact the accuracy of $c(P,T)$ to a slightly greater degree. In the temperature regions where $\frac{\partial c}{\partial T}$ is maximized and equal to ~ 4 m/s/K, the accuracy of the determined sound speed is near 0.3%.

Figure 4 presents a plot of the percent difference between the experimental and theoretical data sets $((\text{measured}-\text{IAPWS})/\text{measured} \times 100)$. Of the 203 sound speeds measured here, 95% were within 0.4% of the IAPWS-IF97 predicted sound speeds. The IAPWS-IF97 standard reports an uncertainty of 0.3-0.4% for sound speed in this P - T space. This corresponds to an absolute uncertainty of ~ 4 m/s for the sound speeds considered here. The IAPWS-IF97 estimates the uncertainty in its calculations based on the estimated uncertainties in the experimental data used to determine the Gibbs free energy basic equation described above.²² Of the more discrepant sound speeds in Fig. 4, many are at temperatures between 400 and 425 K, at all pressures. These 0.3-0.4% differences can be due either to inaccuracies in the temperature measurement, uncertainties in the IAPWS sound speeds, or likely, a combination of both of these factors.

B. Determined B/A

Figure 5 compares the values for B/A determined in this work with those available in the literature at laboratory ambient pressure and at temperatures up to 360 K. As seen in Fig. 5, the room temperature and pressure B/A value of 4.6 found in this work agrees well with most of the values available in the literature. The values of B/A extracted from the measured sound speeds over the entire temperature and pressure range are tabulated in the [Supplementary Material](#). The value of B/A generally trends upward with both pressure and temperature. At the highest temperatures and pressures considered in this work, the measured sound speeds imply a B/A of ~ 10 , while the sound speeds calculated from IAPWS-IF97 lead to a B/A of 7.5. Both data sets show that water is significantly more nonlinear at higher temperatures and pressures, an important result for the development of nonlinear acoustics-based technologies for harsh environments.

Of the ten B/A values determined in this work and plotted in Fig. 5, eight of them agree with that calculated from the IAPWS standard to within 10% (denoted by error bars) which is the uncertainty typically reported by other authors for this parameter. The agreement of the B/A values extracted in this work are compared to those extracted from the IAPWS sound speeds as a percent difference in Fig. 6 over the entire temperature and pressure range. While most previous authors

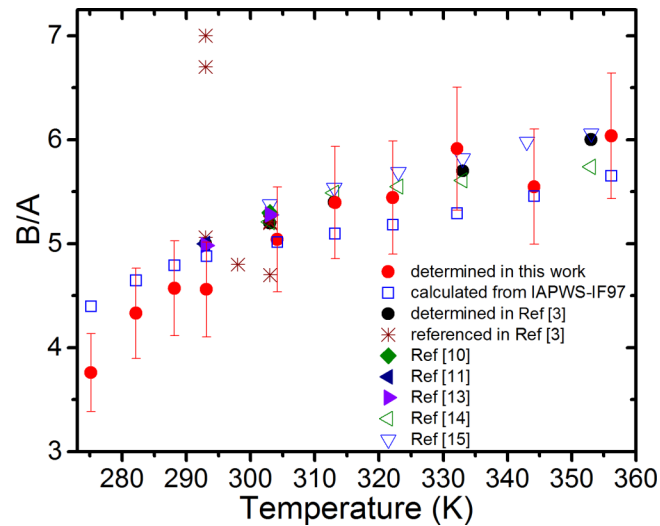


FIG. 5. B/A values for water at ambient pressure up to 356 K from this work compared to available literature values. The error bars on the experimental data from this work denote $\pm 10\%$, a commonly referenced uncertainty in experimentally determined B/A values.

have reported an uncertainty in B/A of 10%, we believe this number likely underestimates the true uncertainty and believe that a discussion of this is warranted.

The slightly low value of B/A at 273 K derived from the SFAI measured sound speeds, as well as the two literature values of $B/A > 6.5$ at room temperature (see Fig. 5) suggest that the commonly quoted 10% uncertainty in B/A is likely overly optimistic. Comparison of Figures 4 & 6 lend further evidence to suggest the uncertainty in B/A is larger than 10%. In Fig. 4, the mean of the absolute difference in sound speed between SFAI measured and IAPWS calculated is only 0.2%; the mean of the absolute difference in B/A determined from these same two data sets, 13%, is significantly larger. It should also be noted that the median of the absolute difference between experimental and predicted B/A values in Fig. 6 is 7%, indicating that the mean is appreciably affected by some of the more outlying points near the perimeter of the P - T space. Because B/A is calculated from derivative quantities, small changes in the underlying physical property (i.e. sound speed) are amplified. As noted above, for water, $(B/A)''$ in Eqn. (2) contributes only $\sim 5\%$ of the total value of B/A ; B/A is thus extremely sensitive to the determination of $\frac{\partial c}{\partial P}$. The need to determine $\frac{\partial c}{\partial P}$ as accurately as

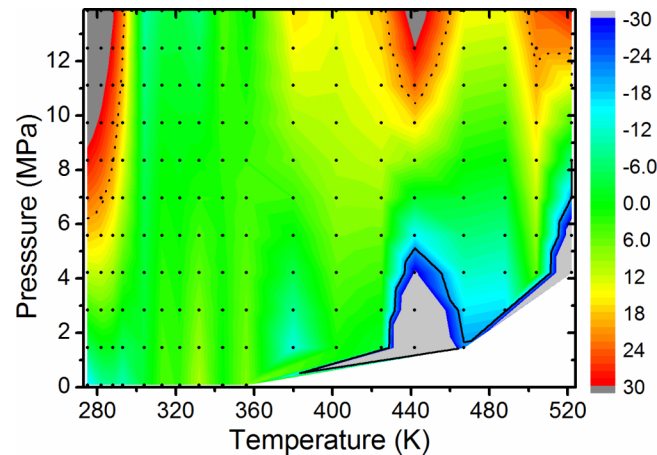


FIG. 6. The difference between B/A values calculated from measured sound speeds and those calculated from IAPWS-IF97, expressed as a percent of the measured values. The solid and dashed lines mark the -20% and 20% contours, respectively.

possible justifies the decision not to include 2σ outliers in the calculation of $\frac{\partial c}{\partial P}$ as described in Section IV. As mentioned above, the speed of sound in water changes by only about 20 m/s over the pressure range considered here. A 2 m/s net error in sound speed over this range thus directly contributes a 9.5% error in B/A . The uncertainty of 4 m/s in the IAPWS-IF97 international standard thus implies an uncertainty approaching 20% in B/A . Of the 185 B/A values extracted here, 78% agree with the IAPWS calculated values to within 20% (Fig. 6). The points in greater disagreement are all found along the boundaries of the data collection P - T space (i.e. at the highest or lowest pressures and temperatures) and are believed to be attributable to edge effects of polynomial fitting as discussed above.

VI. CONCLUSIONS

The measurement of sound speed in liquid water at temperatures from 275 to 523 K and at pressures between laboratory ambient and 14 MPa has been reported. All experimentally measured sound speeds were found to be within 1% of those calculated from the IAPWS-IF97 international standard, with 95% of measured data points being within 0.4% of the predicted sound speeds. The acoustic nonlinearity parameter, B/A , was calculated from both the measured and predicted data set at all temperatures and pressures for which sound speeds were measured. The experimental and IAPWS-IF97 predicted B/A values were in general agreement, particularly at moderate temperatures and pressures where polynomial fitting most accurately captures the true temperature and pressure behavior of the sound speed. The maximum value of B/A determined from measured sound speeds was close to 10 and the IAPWS-IF97 sound speeds led to a B/A near 7.5.

SUPPLEMENTARY MATERIAL

See [supplementary material](#) for tabulated values of all measured sound speeds and determined B/A values.

ACKNOWLEDGEMENT

This work was supported by the U.S. DOE under award # AID 18832. The authors thank Eric Chisolm of Los Alamos National Laboratory for valuable discussions.

- ¹ C. T. Chen, R. A. Fine, and F. J. Millero, "Equation of State of Pure Water Determined from Sound Speeds," *Journal of Chemical Physics* **66**, 2142-2144 (1977).
- ² S. Wiryana, L. J. Slutsky, and J. M. Brown, "The equation of state of water to 200 degrees C and 3.5 GPa: model potentials and the experimental pressure scale," *Earth and Planetary Science Letters* **163**, 123-130 (Nov 1998).
- ³ R. T. Beyer, "Parameter of Nonlinearity in Fluids," *Journal of the Acoustical Society of America* **32**, 719-721 (1960).
- ⁴ A. B. Coppens, R. T. Beyer, M. B. Seiden, J. Donohue, F. Guepin, R. H. Hodson *et al.*, "Parameter of Nonlinearity in Fluids .2.," *Journal of the Acoustical Society of America* **38**, 797-804 (1965).
- ⁵ L. Bjorno, "Characterization of Biological Media by Means of Their Nonlinearity," *Ultrasonics* **24**, 254-259 (Sep 1986).
- ⁶ F. Dunn, W. K. Law, and L. A. Frizzell, "Nonlinear ultrasonic wave propagation in biological media," IEEE Ultrasonic Symposium Proceedings (1981).
- ⁷ W. K. Law, L. A. Frizzell, and F. Dunn, "Determination of the Nonlinearity Parameter B/A of Biological Media," *Ultrasound in Medicine and Biology* **11**, 307-318 (1985).
- ⁸ F. Prieur, S. P. Nasholm, A. Austeng, F. Tichy, and S. Holm, "Feasibility of Second Harmonic Imaging in Active Sonar: Measurements and Simulations," *IEEE Journal of Oceanic Engineering* **37**, 467-477 (Jul 2012).
- ⁹ K. D. Wallace, C. W. Lloyd, M. R. Holland, and J. G. Miller, "Finite amplitude measurements of the nonlinear parameter B/A for liquid mixtures spanning a range relevant to tissue harmonic mode," *Ultrasound in Medicine and Biology* **33**, 620-629 (Apr 2007).
- ¹⁰ W. K. Law, L. A. Frizzell, and F. Dunn, "Comparison of Thermodynamic and Finite-Amplitude Methods of B/A Measurement in Biological-Materials," *Journal of the Acoustical Society of America* **74**, 1295-1297 (1983).
- ¹¹ C. Pantea, C. F. Osterhoudt, and D. N. Sinha, "Determination of acoustical nonlinear parameter beta of water using the finite amplitude method," *Ultrasonics* **53**, 1012-1019 (Jul 2013).
- ¹² J. R. Davies, J. Tapson, and B. J. P. Mortimer, "A novel phase locked cavity resonator for B/A measurements in fluids," *Ultrasonics* **38**, 284-291 (Mar 2000).
- ¹³ E. C. Everbach and R. E. Apfel, "An interferometric technique for B/A measurement," *Journal of the Acoustical Society of America* **98**, 3428-3438 (Dec 1995).

- ¹⁴ Hagelber Mp, G. Holton, and S. Kao, "Calculation of B/A for Water from Measurements of Ultrasonic Velocity Versus Temperature and Pressure to 10000 Kg/Cm²," *Journal of the Acoustical Society of America* **41**, 564-567 (1967).
- ¹⁵ F. Plantier, J. L. Daridon, and B. Lagourette, "Measurement of the B/A nonlinearity parameter under high pressure: Application to water," *Journal of the Acoustical Society of America* **111**, 707-715, Feb 2002.
- ¹⁶ Z. Zhu, M. S. Roos, W. N. Cobb, and K. Jensen, "Determination of the Acoustic Nonlinearity Parameter B/A from Phase Measurements," *Journal of the Acoustical Society of America* **74**, 1518-1521 (1983).
- ¹⁷ J. W. Tester, B. J. Anderson, A. S. Batchelor, D. D. Blackwell, R. D. E. M. Drake, J. Garnish *et al.*, *The Future of Geothermal Energy: Impact of Enhanced Geothermal Systems (EGS) on the United States in the 21st Century* (Massachusetts Institute of Technology, 2006).
- ¹⁸ D. N. Sinha and G. Kaduchak, "Noninvasive determination of sound speed and attenuation in liquids," in *Experimental Methods in the Physical Sciences*, edited by H. E. B. Moises Levy and S. Richard (Academic Press, 2001), Vol. 39, pp. 307-333.
- ¹⁹ L. E. Kinsler, A. R. Frey, A. B. Coppens, and J. V. Sanders, *Fundamentals of Acoustics*, 4th ed. (2000).
- ²⁰ B. T. Sturtevant, C. Pantea, and D. N. Sinha, "An Acoustic Resonance Measurement Cell for Liquid Property Determinations up to 250°C," *Rev. Sci. Instrum.* **83**, 115106 (2012).
- ²¹ J. F. Shackelford and W. Alexander, "Thermal Properties of Materials," in *Materials Science and Engineering Handbook* (CRC Press, Boca Raton, FL, 2001).
- ²² W. Wagner and H.-J. Kretzschmar, *International Steam Tables: Properties of Water and Steam Based on the Industrial Formulation IAPWS-IF97*, 2nd ed. (Springer-Verlag, Berlin, 2008).
- ²³ W. Wagner and A. Pruss, "The IAPWS formulation 1995 for the thermodynamic properties of ordinary water substance for general and scientific use," *Journal of Physical and Chemical Reference Data* **31**, 387-535, June 2002.
- ²⁴ The reader should be aware of a typographical error in Eqn. 5 of Ref. 3 where an extra ρ is included in the denominator of the B/A term. Reference 4 also mentions this.